A Review on Friction Stir Welding of Steel

A. Pradeep

Department of Metallurgical and Materials Engineering, National Institute of Technology, Tiruchirapalli – 620015, Tamilnadu, India

Abstract—Friction stir welding is a solid state welding technology used for welding low melting point metals, such as Al, Mg and its alloys. Later welding was conducted on dissimilar metals which also produced a better defect free joint. Tool design and welding parameters contributes a major role for producing a better weld. Material flow and friction heat are the factors that the internal factor for the formation of weld. At present the research on Friction stir welding on steel is concentrated because of the major use of steels in industries rather than other metals. This paper gives the review of basic concepts of Friction Stir Welding on tool design, mode of metal transfer and process parameters. Further the extensive application of Friction Stir welding on steel is discussed in this study. The mechanical and metallurgical properties on the steel welded material are also focussed.

Keywords—Steels, Tool design, Metal transfer, Microstructure, Tensile strength.

I.   INTRODUCTION

Friction-stir welding (FSW) was patented by Thomas.et.al in 1991. The Welding Institute (TWI) of UK did experiments initially on aluminium and its alloys [1-3]. Magnesium and its alloys were later performed with FSW. Since both the materials have low melting point the FSW is easier to perform and being light weight in advantage they have been widely used in many industries such as automobile and aeronautical industries [15]. The tool is made up of a shoulder and pin. The rotating tool is plunged along the intersection of two metal plates which are rigidly fixed on a backing plate as shown in the Fig.1. When the upper surface of the plates comes in contact with the shoulder surface the friction is developed. Plastic deformation of metal occurs at the joint area along the weld direction. This is influenced by the combined action of shoulder and pin. The pin produces a stirring action at the intersection region and then produces the transfer of metal from the advancing side to retreating side and vice – versa [1-9].

The side of half plate which faces the clockwise direction of rotation of tool along the welding direction is called the advancing side while the other side is called retreating side. It is found that in most of the cases the hardness of retreating side is lower than the advancing side. This is due to the thermal cycles making repeated material transfer to advancing side gives more refined grains [5-11]. The major types of joints are butt joint, lap joint and fillet joint. The schematic illustration of friction stir welding process shown in Fig.1 is a butt type of joint ,while the other type of joints are square butt, edge butt, T butt joint, lap joint, multiple lap joint, T lap joint, and fillet joint as shown in the Fig.2. The most widely used type of joints is butt joint and lap joint. In a butt weld the half plates are placed adjacent to each other while in lap joint the plates are placed one above the other where as in fillet joint the plates are placed in right angles to each other.

A typical macrostructure of FSW weld showing four distinct zones namely base metal (BM), heat-affected zone (HAZ), thermo mechanically affected zone (TMAZ) and Weld nugget (WN) as shown in the Fig.3. Swirl zone (SWZ) is formed mainly due to the thermally induced surface oxidation during welding [4].TMAZ zone is formed due to thermo mechanical cycles and HAZ is the zone which is affected by the frictional heat produced by the shoulder. WN is the region formed due to the stirring action of the pin. Frictional heat produced by the tool makes the plastic deformation of material and grain boundary sliding. Excessive heat formation leads to tool wear which results in loss of material in the tool. Loss of tool material will be formed as an inclusion in the weld region. Feed rate, material flow and heat transfer favors the tool wear to emerge along the weld direction. Tool wear can be reduced by preheating the work piece [6] and by choosing appropriate tool material for the particular work piece.

II.   FRICTION STIR WELDING TOOL

The FSW is emerged from a concept of drilling and hence the tool was initially used with threaded pin. The compaction of plasticized material is given by the bottom of the tool shoulder and prevents the material from escaping. The shoulder have different profile such as flat, concave, smooth or grooved, with concentric or spiral grooves[5]. A concave shoulder has the advantage over flat shoulder because of directing material flow to the centre close the pin. A Grooved bottom has the same effect instead of smooth bottom. Based on the thickness of the plates to be welded the application of tool pin profile varies. The different shapes of tool profile are Cylindrical threaded pin tapered pin, flared-triflute pin as shown in Fig.4. For a commercial aluminium plate tool shape of cylindrical pin having both pin with threaded and without threaded can be applied. The formation of friction stir welded joints is mainly depended on the tool shapes and size. For a thickness of 12mm cylindrical pin shapes are recommended while thickness more than 12mm tapered or triflute shape are recommended [3,11]. The tapered pin or oval cross section makes reduction in probe volume (static volume), allowing one to achieve a suitable swept volume (dynamic volume) to static volume ratio. The greater this ratio, the greater will be the path for material flow and plastic deformation [5, 11, 14]. When compared to butt weld lap weld oxide disruption at the sheet

interface is possible. So tools solving this purpose should be used. Flared-Triflute is allows the dynamic to static volume ratio to be increased, which in turn improves the weld quality [5, 11].

Improving the geometry of a tool can give a good weld. Complex geometry namely triflute was performed in a lap joint which gave a better weld formation than simple geometry. The flow of material was found to be more at the bottom of the shoulder and the pin stirring action is more powerful than the simple geometry [16]. Fig.5 (a) shows a simple geometry where the flow is limited where as in complex geometry (triflute) the flow patterns are more crowded at the shoulder and pin as shown in the Fig.5 (b).

The tool with the pin and shoulder affects the material flow pattern. Heat generation and plastic flow are influenced by the better tool design, which in turn favors the uniformity of material flow along the weld direction. It is evident from the previous experiments conducted by TWI that the tapered pin with threaded portion can give more velocities at vertical direction. This will favor the material flow and makes a uniform distribution of plasticized material throughout the weld line [5]. The tapered or cylindrical pin without screw threads produces defects in the TMAZ (Thermo mechanically affected zone), whereas with the screw threads defect free welds were obtained. The flow of materials from the advancing side to retreating side results in insufficient filling of material in advancing side there by leading to a wormhole defect [19-23]. Considering the flow of material advancing towards the retreating side creating defects, an effective way of mixing of material flow equally on both sides without defect can be given by a conical pin [36, 39].

III. TWO MODES OF METAL TRANSFER

Arbegast.et.al suggested five conventional FSW working zones namely preheat zone, initial deformation zone, extrusion zone, forging zone, and post heat/cool down zone [7] as depicted in the Fig.6. The term pre heat itself denotes heating to prior condition and here it is the region of neighbor near to the edge of the shoulder circumference. As the friction heat is developed by the shoulder some amount of heat is transferred along the welding direction, which is a pre heat condition for the weld to progress. Based on the traverse speed and weld metal thermal property the amount of pre heat prevails. In the initial deformation zone the material is heated to plastic deformation stage. The material flow is influenced at the shoulder bottom and pin. Extrusion zone is due to the stirring action of the pin. The material is stirred from the advancing side to the retreating side. Depending on the stress concentration around the pin and temperature distribution, the width of the extrusion zone varies. In the forging zone the material from both sides are mixed well at plastic deformation condition. Based on the feed rate and rotating speed the effect of extrusion is followed by this zone. The final zone is the cooling after forged zone, in which the stirred material is made to set in a well mixed state. The tensile property of the weld is influenced based on the cooling rate.

First mode of metal transfer is by shoulder while the second mode of metal transfer is due to pin. When the tool rotates the shoulder touches the work piece, thereby friction heat is produced and plastic deformation occurs at the weld zone [24]. When the material flow takes place around the region of the shoulder and pin, the compaction of material is mainly due to the shoulder and this influences the first mode of metal transfer. This will eliminate the formation of defect in weld zone, thereby increasing its tensile property [1, 25]. Extrusion of metal flow is influenced by the stirring action of the pin. Layer by layer material flow takes place at the top region while onion ring pattern is observed below the layers as shown in the Fig.7 [9].

First mode of metal transfer is influenced by the movement of material from the advancing side to retreating side for every rotation of tool leading to the formation of layers one below the other. Second mode of metal transfer is a combined effect of both material flow layer by layer and extrusion of material in plasticized condition [24, 25]. When macro structural observation on the specimen is carried out perpendicular to the weld direction concentric ring patterns were observed. The structure resembles the onion ring pattern and hence the mechanism of flow patter is named as "onion ring". The combined effect of two modes of metal transfer results to produce the onion rings [9, 33]. The extrusion of material at each rotation of the tool pin and compaction of shoulder together creates the geometry of onion rings [26, 27] as shown in the Fig.8. Two modes of metal transfer are responsible for the formation of onion rings [9- 27].

Even the base material and welding parameters will contribute the formation of onion rings. In some welds the intermetallic particles combine with the base material and diffuse to form onion ring pattern [28-32]. It was found that in some micro regions of a lap-butt weld did for different offset values; three flow patterns were observed namely turbulent flow, laminar flow and circumfluence flow [16]. When pins off-set value (t) is taken as zero the material flow pattern shows a circumfluence flow and an interfacial gap is clearly visible at the retreating side as shown in Fig.9 (a). Even when a pin offset value of 0.5 is used it is observed that circumfluence flow of pattern is observed but with very minute interfacial gap as shown in Fig.9 (b). The microscopic image of circumfluence is shown in the Fig.10 (a), which is influenced by the action of pin and onion ring structure is formed in the nugget zone.

When pin offset of 1 mm is used, turbulent and laminar flow is observed with interfacial gap more than the weld of pin offset value of t =0.5, as shown in the Fig.9 (c) . Laminar and turbulent flow is observed in the nugget zone as shown in the Fig.9(b) &(c) respectively and this material flow is produced by the effect of shoulder. When larger tool is used, the flow of material for each rotation of tool gets reduced and hence there is reduction of formation of onion ring pattern [9, 27-33]. By using the traces of flow visualization, it is noticed that the material move to retreating side in the transitional zone as the tool advances the nugget zone [37, 38] tending to create a concentric circle for each rotation when tool rotates. During the rotation of the tool the velocity will be high near the tool shoulder edge and then it gradually decreases to the layer below. Thus the compaction created by the shoulder and extrusion of pin is responsible for the formation of onion rings.

IV. EFFECT OF FSW PROCESS PARAMETER

The process parameter which influences the formation of weld joint are tool rotational speed, traverse speed, tool tilt angle, force exerted by the tool and plunge depth. When the process parameter is properly used defects can be minimized. These parameters and material properties are responsible for the temperature profiles, cooling rate and torque exerted by the

tool. When compared to conventional fusion welding process the peak temperature and diffusion of heat source is significantly low. With respect to axial pressure, when the rotating speed increases the peak temperature also rises in the weld zone [40]. Even the torque increases with increase in rotation speed when tool tilt angle, friction coefficient, and traverse speed are kept constant [41]. Due to the action of rotating speed the relative velocity between the tool and material increases thereby the axial pressure along the weld distance increases. When traverse speed was considered and other variables are kept constant, the torque got slightly increased. This shows that traverse speed has less effect on the peak temperature and torque when compared to rotating speed. Even though the welding is based on alloy compounds, with crack or void increases with traverse speed [42]. For thickness up to 4mm when the tool is tilted at an angle of 1° the weld strength is found to good. When the tool tilt angle is further increased void formation occurred in the weld zone. Because of reduction in shear strength and greater strain rate, the defect is about to occur. Further with increase in the thickness of weld plate the tool tilt angle should be increased [43, 44].

The force exerted by the tool between the intersections of weld plate should be considered during welding because when the axial force is high tool erosion and tool breakage might occur at extreme cases. By using dynamometer the force on tool can be calculated and this could be useful to predict the defect formation [45]. When force is exerted by the tool, internal pressure is created at the bottom of tool shoulder. When the pressure gets higher the material is removed as flash and the joint area gets thinner, whereas when the pressure is low void occurs. At low traverse speed, weld is performed on a stainless plate and the peak temperature distribution on advancing side and retreating side were calculated. It is found that the peak temperature at the advancing side is more than the retreating side [46, 47]. However this result is similar to most of the alloys of aluminum [48-50]. At the edge of the tool shoulder the peak temperature will be high. Thermal cycles might affect the microstructure of welded materials. Sometimes it leads precipitation growth and dissolution of grain [51-54]. Cooling rates also affects the grain size particularly in age hardenable alloys. In high carbon steels the cooling rate influences the formation of martensite. When the traverse speed decreases, the cooling rate also decreases with the decrease in peak temperature. In order to avoid martensite formation low traverse speed with low rotational speed should be processed [55-57].

Excess flash formation should be prevented, because of greater plunge depth the useful material might be removed and makes the joint thinner. In ferritic stainless steel, inspection was carried on flash formation and the macroscopic images are analyzed and it produced different defects [58]. Tunnel defect, pinhole defect and root defect were observed with respect to tool rotation speed, traverse speed and shoulder diameter as shown in the Table.1. Sensitivity analysis was performed on these process parameters and found that welding speed has greater influence on tensile strength and impact toughness, followed by rotational speed and shoulder diameter. Excess flash formation is a form of defect produced because of surface overheating between the tool shoulder and work material [59, 60].

With an increase in traverse speed and keeping the rotation speed constant, the wormhole will initiate near the bottom of the bottom because of inadequate material flow [59]. The ratio of traverse speed to rotational speed is an important factor to be considered for the propagation of wormhole. If higher the ratio of traverse speed to rotational speed, then easier the formation of wormhole [61, 62]. Tool profiles may also contribute in the formation of porosity and affects the material flow pattern. The defect propagation can be a combination of both tool profile and process parameter. When five pin profiles (straight cylindrical, tapered cylindrical, threaded cylindrical, triangular and square) were used with a constant rotating speed, a square tool pin profile gave less defect when compared to other profiles [63]. Modeling has been done on cryogenic cooling when it is applied on the welded joint immediately after welding and found that dislocations were found at the grain boundaries [64-66]. It is concluded that the welding process parameter and tool profiles has its effect to decide the strength of weld and its defect [63-70].

V. FSW OF STEEL

In recent years, the research is concentrated on FSW of steels because of the major application of steels in the industries. When compared to aluminium and its alloys, FSW process performed on steels are limited. The tool material for welding is a major constraint for welding steels. At present the most commonly used tool material for steels are polycrystalline cubic boron nitride (PCBN) and tungsten based tools. Being cost effective and too brittle, PCBN tools are be replaced with tungsten alloy tools which have been used in many early welds [71, 72]. The tool material should have higher melting temperature than the work material. If the case is steel, the steel itself poses high melting temperature. So selecting a proper tool for welding steel is a challenging task. When compared to aluminum the grades of steel and its alloys are plenty. For a single application many grades of steels may come into focus. At this critical situation, appropriate steel which will satisfy the most of the need should be selected. Further commercial welding process such as TIG, Arc welding is used in most of the industries. The application of FSW is an eco technology and since now it is used welding steels [73, 74]. The microstructure and phase transformation of steels in FSW have not yet deeply studied and only based on hardness test, impact toughness and tensile strength the mechanical properties of steel are optimized. Texture, fracture toughness, fatigue strength and elongation under load properties need deeper characterization study in FSW of steels [75-78]. FSW being a solid state welding process and its application on welding of steel have many advantages such as elimination of welding fumes and hydrogen cracking in steels; minimal distortion and residual stress will help to weld thick section of components [79-81]. Table.2 is an update of FSW parameters and tool materials for FSW of steels predicted by Mishra.et.al [15]. FSW welding of SK5 steel was performed with and without the application of gas torch. This was done to control the cooling rate during the process [82]. When compared to IF steels, S12C and S35C are affected by welding conditions. This is evident from the microstructure, in the ferrite-austenite two-phase region where the microstructure is refined. By increasing the traverse speed the strength of the S12C and S35C steel joints got increased [83]. The strength of the weld is tested for tensile and impact, and the tensile strength was found to more than the base Metal [84]. FSW is performed on M190 steel, the rate of heat input and cooling rate during welding is related from the previously available empirical relationships. The mechanical properties of the joints can be deeply understood from the micro and macro structural analysis [85]. From the

micro structural observation it is found that the TMAZ zone seen in aluminium alloys is not observed in steels [89, 91]. But the micro structural observation seen in 304 and 306 grades of steel confirmed the presence of TMAZ zone [85, 95-97]. During FSW process inert gas like argon atmosphere is provided in a closed surface in order to prevent oxidation of steel [87, 89, and 97]. The weld zone were found to exceed a peak temperature of 1000°C [94], and in the HAZ zone, fine pearlites are randomly distributed in the equiaxed ferrite grains [89]. When the plate thickness of steel is less than 6mm a single pass of weld is efficient, but when the plate thickness is more than 6mm two passes are necessary to produce an efficient weld [87]. Pre heating the steel plates before the welding process begins can make 6mm plate of steel in single pass [89].

A. Macro And Micro Structural Studies

A typical weld region of AISI 1018 steel contains five distinct regions namely the nugget zone, swirl zone, thermo mechanical affected zone (TMAZ), fine grained heat affected zone (FGHAZ) and coarse grained heat affected zone (CGHAZ) [84] as shown in the Fig.11.In the stir zone ferrite/carbide aggregate appears to be fine pearlite and some inclusions of tungsten particles from tool were observed. It is evident from the micro structural studies that peak temperature during welding reached into the austenite phase, allowing for appreciable grain growth at the centre of stir zone, which resulted in elongated mixed structure of polygonal ferrite and pearlite as depicted in Fig. 11 (c). Stir zone and TMAZ zone experience both temperature and deformation. HAZ experiences only thermal cycles and shows two distinct zones, the inner HAZ zone and the outer HAZ zone. Inner HAZ zone has a refined ferrite structure with small amounts of pearlite. Outer HAZ zone is located between the inner HAZ region and the unaffected base metal, which has an equiaxed grain structure with a grain size substantially larger than that of the inner HAZ and very similar to that of the base metal as shown in the Fig.11 (f). The outer HAZ, between the inner HAZ and the unaffected base metal, had an equiaxed grain structure with a grain size substantially larger than the inner HAZ and slightly larger than the base metal. Although the TMAZ underwent plastic deformation, recrystallization did not occur in this zone due to insufficient strain rate, and hence the TMAZ zone is not clearly visible. The grains in TMAZ contains sub – boundaries of high density thereby the rate of dissolution depends on the thermal cycle experienced by TMAZ.

Ghosh.et.al describes that for a lap weld of high strength steel , the weld nugget consist of three distinct regions 'I', 'II' and 'III' [85] as hown in Fig.12. The region 'I' is influenced by the tool shoulder and region 'II' is influenced by the pin. The effect of tool periphery influences region 'IV'. Region 'III' is a mixed zone of regions 'II' and 'IV'. Region 'IV' and 'V' represents HAZ zone 1 and HAZ zone respectively. The dotted lines are the region expanded due to the high heat input and cooling rate. The microstructure in the weld nugget at normal cooling shows ferrite and pearlite, but when the cooling rate is increased weld nugget shows martensite. HAZ zone 1 shows polygonal ferrite structure, while HAZ zone 2 shows higher hardness than HAZ zone 1 containing tempered martensite. It is evident that TMAZ zone is not observed in the weld structure [84, 85]. But in FSW of 304L and 316L steels partial recrystallization in the TMAZ is observed [87]. In the HAZ zone of HSLA -65 steel weld, Widmanstatten ferrite and ferrite carbide aggregates were found in the stir zone [89]. Whereas in DH-36 steel, bainite and martensite structures were observed in the nugget zone and in HAZ zone small amounts of pearlite are distributed [90]. FSW weld of C-Mn steel shows TMAZ zone with fine-grained structures near the stir zone. The base metal consists of allotriomorphic ferrite and pearlite. Equiaxed prior austenite grain structures were seen in the TMAZ [91]. For a high carbon steel at A_3 temperature the ferrite structure and globular cementite structure were fully transformed to an austenite structure during FSW, and after welding the material underwent solid-state transformation from austenite structure to martensite structure, but in HAZ zone martensite is not observed. When an external heat is given by gas torch the carbon atoms diffuse out during the cooling and contribute the formation of martensite [82]. Deformation in HAZ might increase the amount of austenite grain per unit volume .This would lead to a corresponding large increase in the grain boundary nucleation rate of allotriomorphic ferrite [96-98]. Heat input provided the best correlation with post-friction stir weld microstructures. Heat input exhibits a linear relationship with ferrite grain size and bainite lath size. Ferrite grain size and bainite lath size both increased 150% with an increase in heat input of 2.27 kJ/mm [86].

B. Mechanical Properties of FSW Steels

Basically it is expected that the hardness of the welded region to be higher than the base metal, irrespective of the welding condition. Chemical composition and Hardness predicted in FSW of steels are listed in Table.3. Don-Hyun Choi.et.al predicted the hardness for SK5 steel [82]. The base metal with ferrite and globular cementite structure shows a hardness of about 200 HV [83]. After FSW, if the case A without gas torch as external heat source is used, then the average hardness in the weld centre is about 850 HV. In the case B with gas torch, its average hardness is predicted as about 750 HV. This variation was related with the different volume fraction of martensite structure: the case B had less martensite structure than the case A, which lowered its average hardness. In the HAZ, the hardness was drastically increased from the 200 HV of the base metal to a range of 750–850 HV in the weld center of both cases A and B. The effect of the external heat on the hardness profile was not negligible. For the IF steel, the welding speed does not significantly affect the hardness profiles of the joints, while for the S12C steel, the higher the welding speed (the smaller heat input), the greater the hardness [83]. However for S35C, the greatest hardness was obtained with the medium heat input (near 200 mm/min), and a significant decrease in the heat input induced the decreasing hardness. When FSW is performed on AISI1018 steel, the hardness in the stir zone varies from 146 to 492 HV, which is greater than the base metal hardness of 140HV. The higher hardness is due to the presence of very fine equiaxed grains of ferrite and few grains of pearlite as depicted in the Fig. 11 (b) [84]. M190 martensitic steel possesses a hardness of 160VHN with coarse ferrite and pearlite [85].

The weld nugget microstructure shows hardness in the range of 303–357 VHN with martensite structure. The area in contact with shoulder contained a thin band of tempered martensite with reduced hardness of 277VHN. The region close to the faying surfaces of the sheet exhibited a narrow ferrite layer with a sudden drop in hardness. Hardness of martensite depends on carbon content, and for 0.2% carbon steel the hardness may reach up to 540 VHN. Apart from the cooling due to

the process, the forced air cooling became effective from the edge of the shoulder as the tool moved. However, residual heat flow from inside the nugget caused tempering of the upper layer. At the bottom, the forced air cooling effect was minimal and heat extraction was primarily through conduction to the bottom plate at a much lower rate; so large polygonal ferrite formed along with pearlite, and the result was low hardness values. Peak hardness of martensitic region showed a maximum of 560 VHN. They have indicated that martensite formed at a relatively slower cooling rate exhibited higher hardness than martensite formed at a higher cooling rate. The higher hardness was attributed to the precipitation of carbides at lath boundary. In the case of M190 steel, the microalloying element Ti was responsible for carbide precipitation during cooling. The alloy carbide precipitation was responsible for higher hardness of martensite peak hardness remained close, because the hardness of martensite remains more or less unchanged beyond a certain cooling rate, depending on the steel composition. HAZ zone 1 contained predominantly polygonal ferrite with maximum drop in microhardness, and HAZ zone 2 consisted of tempered martensite with relatively higher microhardness than HAZ zone 1. Most of the FSW steel welds are evident that TMAZ zone is not visible in the weld zone [82-86], but in some cases the TMAZ zone can be differentiated from the HAZ zone [72-75,83]. Even though the TMAZ zone is differentiated from the HAZ zone, there is no vast difference in structure between these zones [79-81]. Peak temperatures are mostly occurred in the regions of TMAZ zone [48, 72, and 83].

In SK5 steel the base metal poses an ultimate tensile strength of 610 MPa. Tensile specimens were fractured at the base metal [82]. The tensile strength of cases A and B was the same as that of the base metal. The percentage of elongation in both cases A and B was found to be lower than the base metal with the elongation of 12% and 13% respectively. This might be due to the strength of the weld greater than the base metal. When the traverse speed exceeds more than 200mm/min, the tensile strength of IF steels, S12C and S35C steels got decreased [83]. Fine grained Ferrite with pearlite structure is observed in the Weld regions making the tensile strength higher, because the peak temperature is in the region of ferrite- austenite two phase region [83,101]. When shoulder diameter 20mm is used for welding AISI 409M ferritic stainless Steel of 4mm thick, highest tensile strength is achieved but the impact toughness decreased with increase in shoulder diameter [58]. This is mainly due to the formation and uneven distribution of martensite in the weld region.

AISI 1018 steel with a thickness of 5mm was welded and tensile specimens were prepared as per the ASTM E8M-04 guidelines [84]. Charpy impact specimens were prepared as per the ASTM E23-04 and hence the notch is placed at the weld region. The fracture was found to occur away from the weld region [92-96] and was analysed in scanning electron microscope. The fractograph shows finer dimple structure than the base metal which is an indication that specimens were failed in ductile manner under the action of tensile loading as shown in the Fig.13. Loading condition during testing had negligible effect over either the joint efficiency or failure distance from weld centre [85]. A small amount of ferrite with pearlite is found in the fracture region of FSW welded M190 martensitic steel. FSW weld of C−Mn steel shows lesser tensile strength than the base metal since the fracture occurred at the HAZ zone [91].

Since FSW is performed on steels an important factor to be considered is corrosion properties. If the weld shows homogeneous electrochemical potential then there is possibility of minimal corrosion, without considering environmental reactions. When salt spray test is conducted on HSLA steel no significant weight loss or tendency to pit is seen [79,102]. Studies research in this relevant field is very limited and should take this property as serious and solutions should be found out. This is because the chemical composition of the weld region is identical to that of the plates. Tool wear in FSW of steels occurs because of high temperature evolved during welding and when tool is plunged into the work plate. When tool is plunged initially into the workpiece, friction occurs between the tool and workpiece [93, 94]. Possibility of removal of tool material at the shoulder edge and deformation tool at high temperature can change the dimension. Tools can be replaced after 1.5-2m after weld [93]. When quenched and tempered C-Mn steel was welded using PCBN tool, very little wear was observed 6m of weld [100]. If the hardness of the tool is high then the nature of brittleness definitely will be higher, so tempered steels with good ductility gives the tool life longer [103]. Tool wear can be controlled by selecting proper tool for welding and most preferably using alloy elements which can withstand high temperature. Dimension and structure of Tool design is also an important factor, which favors tool wear. Even a good tool design with proper process parameter [100,104] can contribute in reducing the tool wear. Preheating the tool and workpiece will improve the weld quality and tool wear will be minimal. Further more research is needed to concentrate in this area, because the cost of tool is also a constraint for performing welding. If the life of tool is limited and needs often replacement, then cost of welding seems to hurdle.

VI.   OUTLOOK AND REMARKS

Friction stir welding being a widespread interest for most of the upcoming researchers in the area of welding, it finds its importance in welding steels. Without the application of steel in industries is unimaginable. As a special interest to review the recent developments in FSW steel welding, this paper gives initially the basic concepts to understand formation of weld and its process parameter which functions to give such a permanent joint. Addressing the review of Mishra.et.al (2005) and Nandan.et.al (2008), this review is restricted to only the developments and improvements in friction stir welding of steels. Two modes of metal transfer is such a understanding concept given by Muthukumaran.et.al (2008), to know deeply about the formation of FSW weld and material flow. It is discussed how the tool design and welding process parameter contributes in the formation of joint between similar and dissimilar welds. Butt and lap joints are the two widely used types of joints. Most of the welds are performed on butt type of joints rather than lap joint because no need of surface preparation, easy to fix, clamp and perform welding. In most of the cases the FSW welding is done with cylindrical threaded pin, but there are very few applications in tapered pin. Tapered threaded pin can give better strength and uniform weld throughout the length of the plate as discussed in tool design. Vertical mixing at high velocity and tool wear can be minimised through this design. Because of tapered pin the pin is plunged smoothly into the intersection area and there are no sharp edges at corner of the pin. As the result says concave shoulder gave joints with better joint strength rather than flat shoulder because of its nature to give more compaction to the deformed material and prevents the material from flash formation and hence flash propagation is greatly reduced. Rotating speed, traverse speed and tilt angle are the majors factors which were found to influence the weld formation more than the other process parameter such as plunge depth, force exerted by the tool, etc.

compared to weld, where the tool rotates perpendicular to the workpiece, when placed at an angle facing the direction gave high strength joint. As discussed when tool tilted at an angle of more than 1° void formation is observed and this condition is for a plate not more than 4mm thickness. The tool tilt angle is based on the thickness of plates to be used. It is observed that in some cases of FSW steel weld TMAZ zone is not seen and in other cases HAZ and TMAZ zones are clearly distinct. TMAZ zone is influenced by both mechanical and thermal cycles, while HAZ zone is influenced by only thermal cycles. Peak temperatures can be seen only in the HAZ zone, due to this hardness in the region will be more. Differentiating TMAZ zone from HAZ zone is most preferably difficult and hence in most of the weld, the region is differentiated as two zones in HAZ viz. HAZ zone 1 and HAZ zone 2. Fatigue life and fracture toughness of FSW steel weld is not explained and studied till yet. When compared to aluminum and its alloys, the characterization study on FSW steels are very less. Only based on the tensile strength and impact toughness, the quality of FSW steel welds are evaluated. Hence more characterization study is needed for deeper knowledge of FSW welds. Corrosion in steel and iron is a natural phenomenon, which occurs at a faster rate than any other metal. Hence alloying element is added, to improve corrosion resistance. Study of corrosive nature in the weld region of FSW of steel is not carried out in any of the previous studies. Further tool wear is an important criterion to be considered before planning for FSW of steel. One practical remedy for controlling the tool wear is preheating the tool and work piece and the other is as said before that selecting a suitable alloying element. Corrosion and tool wear is not only the properties for study, there is lots of characterization study that is need for FSW of steels to undergo and understand.

REFERENCES

[1]. Preetish Sinha, S. Muthukumaran, S.K. Mukherjee. Analysis of first mode of metal transfer in friction stir welded plates by image processing technique. journal of materials processing technology 197 (2008) 17–21.

[2]. S. Muthukumaran & Kumar Pallav & Vikas Kumar Pandey & S. K. Mukherjee. A study on electromagnetic property during friction stir weld failure. International journal of Advanced Manufacturing Technology (2008) 36:249–253.

[3]. Thomas WM, Nicholas ED, Needham JC, Murch MG, Temple-Smith P, Dawes CJ. Friction stir butt welding. International Patent Application No. PCT/GB92/02203; 1991

[4]. Moataz M. Attallah, Hanadi G. Salem. Friction stir welding parameters: a tool for controlling abnormal grain growth during subsequent heat treatment. Materials Science and Engineering A 391 (2005) 51–59

[5]. Thomas WM, Johnson KI, Wiesner CS. Friction stir welding-recent developments in tool and process technologies. Adv Eng Mater 2003;5:485–90.

[6]. Mandal A, Roy P. Modeling the compressive strength of molasses–cement sand system using design of experiments and back propagation neural networks. J Mater Process Technol 2006;180:167–73.

[7]. W.J. Arbegast, in: Z. Jin, A. Beaudoin, T.A. Bieler, B. Radhakrishnan (Eds.), Hot Deformation of Aluminum Alloys III, TMS, Warrendale, PA, USA, 2003, p. 313.

[8]. Su J-Q, Nelson TW, Mishra R, Mahoney M. Microstructural investigation of friction stir welded 7050-T651 aluminium. Acta Mater 2003;51(3):713–29.

[9]. S. Muthukumaran & S. K. Mukherjee. Multi-layered metal flow and formation of onion rings in friction stir welds. International journal of Advanced Manufacturing Technology. (2007). DOI 10.1007/s00170-007-1071-3.

[10]. Mahoney MW, Rhodes CG, Flintoff JG, Spurling RA, Bingel WH. Properties of friction-stir-welded 7075 T651 aluminum. Metall Mater Trans A 1998;29(7):1955–64.

[11]. Thomas, W.M. and Dolby, R. E. 2003, Friction stir welding developments, Proc. 6th Int. Conf. on Trends in Welding Research. Eds. S. A. David, T. DebRoy, J. C. Lippold, H. B. Smartt and J. M. Vitek, pp. 203-211. ASM International.

[12]. Thomas WM, Staines DG, Johnsonand KI, Evans P. Com-stir – compound motion for friction stir welding and machining.Adv Eng Mater 2003;5:273–4.

[13]. Jata KV, Semiatin SL. Continuous dynamic recrystallization during friction stir welding. Scripta Mater 2000;43:743–8.

[14]. Thomas WM. Friction stir welding – recent developments. Mater Sci Forum 2003;426–432:229–36.

[15]. Mishra RS, Ma ZY. Friction stir welding and processing. Mater Sci Eng R: Rep 2005;50(1–2):1–78.

[16]. Bo Li, Yifu Shen. "A feasibility research on friction stir welding of a new-typed lap–butt joint of dissimilar Al alloys". J Mater Design (2011), doi :10.1016/j.matdes.2011.05.033.

[17]. Zhao YH, Lin SB, Qu F, Wu L. Influence of pin geometry on material flow in friction stir welding process. Mater Sci Technol 2006;22:45–50.

[18]. Nandan R, Roy GG, Lienert TJ, DebRoy T. Numerical modelling of 3D plastic flow and heat transfer during friction stir welding of stainless steel. Sci Technol Weld Join 2006;11:526–37.

[19]. Nandan R, Roy GG, Lienert TJ, DebRoy T. Three-dimensional heat and material flow during friction stir welding of mild steel. Acta Mater 2007;55:883–95.

[20]. Colegrove PA, Shercliff HR. Development of Trivex friction stir welding tool. Part 1 – Two-dimensional flow modelling and experimental validation. Sci Technol Weld Join 2004;9:345–51.

[21]. Colegrove PA, Shercliff HR. Development of Trivex friction stir welding tool. Part 2 – Three-dimensional flow modelling. Sci Technol Weld 2004;9:352–61.

[22]. Lienert Jr TJ, Stellwag WL, Grimmett BB, Warke RW. Friction stir welding studies on mild steel. Weld J Res Suppl 2003;82:1s–9s.

[23]. Guerra M, Schmidt C, McClure JC, Murr LE, Nunes AC. Flow patterns during friction stir welding. Mater Charact 2002;49:95–101.

[24]. S. Muthukumaran and S. K. Mukherjee. Two modes of metal flow phenomenon in friction stir welding process. Science and Technology of Welding and Joining 2006 VOL 11 NO 3 337.

[25]. Preetish Sinha & S. Muthukumaran & R. Sivakumar & S. K. Mukherjee. Condition monitoring of first mode of metal transfer in friction stir welding by image processing techniques. International journal of Advanced Manufacturing Technology (2008) 36:484–489.

[26]. Schneider JA, Nunes AC. Characterization of plastic flow and resulting microtextures in a friction stir weld. Metall Mater Trans B 2004;35:777–83.

[27]. Krishnan KN. On the formation of onion rings in friction stir welds. Mater Sci Eng A 2002;327:246–51.

[28]. Attallah MM, Davis CL, Strangwood M. Influence of base metal microstructure on microstructural development in aluminium based alloy friction stir welds. Sci Technol Weld Join 2007;12:361–9.

[29]. Sutton MA, Yang B, Reynolds AP, Taylor R. Microstructural studies of friction stir welds in 2024-T3 aluminum. Mater Sci Eng A 2002;323(1–2):160–6.

[30]. lee WB, Yeon YM, Jung SB. The joint properties of dissimilar formed Al alloys by friction stir welding according to the fixed location of materials. Scripta Mater 2003;49:423–8

[31]. Colligan K. Material flow behavior during friction stir welding of aluminum. Weld J Res Suppl 1999;78:229s–37s

[32]. Kumar A, DebRoy T. Guaranteed fillet weld geometry from heat transfer model and multivariable optimization. Int J Heat Mass Transfer 2004;47(26):5793–806.

[33]. Buffa G, Hua J, Shivpuri R, Fratini L. Design of the friction stir welding tool using the continuum based FEM model. Mater Sci Eng A 2006;419:381–8.

[34]. Boyce DE, Dawson PR, Sidle B, Gnäupel-Herold T. A multiscale methodology for deformation modeling applied to friction stir welded steel. Comput Mater Sci 2006;38:158–75.

[35]. Nandan R, Lienert TJ, DebRoy T. Toward reliable calculations of heat and plastic flow during friction stir welding of Ti– 6Al–4V alloy. Int J Mater Res 2008;99:434–44.

[36]. Seidel TU, Reynolds AP. Two-dimensional friction stir welding process model based on fluid mechanics. Sci Technol Weld Join 2003;8:175–83.

[37]. Schmidt H, Dickerson TL, Hattel J. Material flow in butt friction stir welds in AA2024-T3. Acta Mater 2006;54:1199–209.

[38]. Seidel TU, Reynolds AP. Visualization of the material flow in AA2195 friction-stir welds using a marker insert technique. Metall Mater Trans A 2001;32:2879–84.

[39]. Fratini L, Buffa G, Palmeri D, Hua J, Shivpuri R. Material flow in FSW of AA7075-T6 butt joints: numerical simulations and experimental verifications. Sci Technol Weld Join 2006;11:412–21.

[40]. Sato Y, Urata M, Kokawa H. Parameters controlling microstructure and hardness during friction-stir welding of precipitation-hardenable aluminum alloy 6063. Metall Mater Trans A 2002;33(3):625–35.

[41]. Sellars CM, McTegart WJ. On the mechanism of hot deformation. Acta Metall 1966;14:1136–8.

[42]. Leal R, Loureiro A. Defect formation in friction stir welding of aluminium alloys. Adv Mater Forum II 2004;455–456:299–302.

[43]. Kittipong Kimapong. and Takehiko Watanabe. Effect of Welding Process Parameters on Mechanical Property of FSW Lap Joint between Aluminum Alloy and Steel. Materials Transactions, Vol. 46, No. 10 (2005) pp. 2211 to 2217.

[44]. G. H. Payganeh, N. B. Mostafa Arab, Y. Dadgar Asl, F. A. Ghasemi and M. Saeidi Boroujeni. Effects of friction stir welding process parameters on appearance and strength of polypropylene composite welds. International Journal of the Physical Sciences Vol. 6(19), pp. 4595-4601, 16 September, 2011.

[45]. Hassan KAA, Pragnell PB, Norman AF, Price DA, Williams SW. Effect of welding parameters on nugget zone microstructure and properties in high-strength aluminium alloy friction stir welds. Sci Technol Weld Join 2003;8:257–68.

[46]. Cho JH, Boyce DE, Dawson PR. Modeling strain hardening and texture evolution in friction stir welding of stainless steel. Mater Sci Eng A 2005;398:146–63.

[47]. [47] R.P. Dobriyal , B.K. Dhindaw, S. Muthukumaran, S.K. Mukherjee. Microstructure and properties of friction stir butt-welded AE42 magnesium alloy. Materials Science and Engineering A 477 (2008) 243–249.

[48]. [48] Sato Yutaka S, Kokawa Hiroyuki, Enomoto Masatoshi, Jogan Shigetoshi. Microstructural evolution of 6063 aluminum during friction-stir welding. Metall Mater Trans A 1999;30(9):2429–37.

[49]. Sato Y, Park SHC, Kokawa H. Microstructural factors governing hardness in friction-stir welds of solid-solution-hardened Al alloys. Metall Mater Trans A 2001;32(12):3033–42.

[50]. Liu G, Murr LE, Niou C-S, McClure JC, Vega FR. Microstructural aspects of the friction-stir welding of 6061-T6 aluminum. Scripta Mater 1997;37(3):355–61.

[51]. Roy GG, Nandan R, DebRoy T. Dimensionless correlation to estimate peak temperature during friction stir welding. Sci Technol Weld Join 2006;11:606–8.

[52]. McClure JuC, Tang W, Murr LE, Guo X, Feng Z, Gould JE. A thermal model for friction stir welding. In: Vitek JM, David SA, Johnson JA, Smartt HB, DebRoy T, editors. Trends in welding research. Ohio, USA: ASM International; 1998. p. 590–5.

[53]. Schmidt H, Hattel J. A local model for the thermomechanical conditions in friction stir welding. Modell Simul Mater Sci Eng 2005;13:77–93.

[54]. Nandan R, Prabu B, De A, DebRoy T. Improving reliability of heat transfer and materials flow calculations during friction stir welding of dissimilar aluminum alloys. Weld J 2007;86(10):313s–22s.

[55]. Kumar A, Zhang W, DebRoy T. Improving reliability of modelling heat and fluid flow in complex gas metal arc fillet welds. Part I: An engineering physics model. J Phys D: Appl Phys 2005;38:119–26.

[56]. Kumar A, DebRoy T. Guaranteed fillet weld geometry from heat transfer model and multivariable optimization. Int J Heat Mass Transfer 2004;47(26):5793–806.

[57]. Zienkiewicz OC, Cormeau IC. Visco-plasticity solution by finite-element process. Arch Mech 1972;24:872–89.

[58]. A. K. Lakshminarayanan and V. Balasubramanian. "Understanding the Parameters Controlling Friction Stir Welding of AISI 409M Ferritic Stainless Steel". Met. Mater. Int., Vol. 17, No. 6 (2011), pp. 969~981. doi: 10.1007/s12540-011-6016-6. Published 27 December 2011.

[59]. Kimand YG, Fujii H, Tsumura T, Komazaki T, Nakata K. Three defect types in friction stir welding of aluminium die casting alloys. Mater Sci Eng A 2006;415:250–4.

[60]. Crawford R, Cook GE, Strauss AM, Hartman DA, Stremler MA. Experimental defect analysis and force prediction simulation of high weld pitch friction stir welding. Sci Technol Weld Join 2006;11:657–65.

[61]. Liu HJ, Fujii H, Maeda M, Nogi K. Tensile fracture location characterisation of friction stir welded joints of differen aluminium alloys. J Mater Sci Technol 2004;20:103–5.

[62]. Long X, Khanna SK. Modelling of electrically enhanced friction stir welding process using finite element method. Sci Technol Weld Join 2005;10:482–7.

[63]. Elangovan K, Balasubramanian V. Influences of pin profile and rotational speed of the tool on the formation of friction stir processing zone in AA2219 aluminium alloy. Mater Sci Eng A 2007;459:7–18.

[64]. Paglia CS, Buchheit RG. Microstructure, microchemistry and environmental cracking susceptibility of friction stir welded AA2219-T87. Mater Sci Eng A 2006;429:107–14.

[65]. Okuyucu H, Kurt A, Arcaklloglu E. Artificial neural network application to the friction stir welding of aluminum plates. Mater Des 2007;28:78–84.

[66]. Kamp N, Sullivan A, Thomasl R, Robson JD. Modelling of heterogeneous precipitate distribution evolution during friction stir welding process. Acta Mater 2006;54:2003–14.

[67]. Reynolds AP. Visualisation of material flow in autogenous friction stir welds. Sci Technol Weld Join 2000;5(2):120–4.

[68]. Baillas G, Donne CD. Characterisazion of friction stir welded joints of the aluminium alloy AA 2024-T3 by laser extensometry. Materialprufung 2000;42:236–9.

[69]. Gupta RK, Biju S, Ghosh BR, Sinha PP. Microstructural evolution and properties of friction stir welded aluminium alloy AA2219. Aust Weld J 2007;52:35–9.

[70]. Peel MJ, Steuwer A, Withers PJ, Dickerson T, Shi Q, Shercliff H. Dissimilar friction stir welds in AA5083–AA6082. Part I: Process parameter effects on thermal history and weld properties. Metall Mater Trans A 2006;37(7):2183–93.

[71]. Cui Ling, Fujii Hidetoshi, Tsuji Nobuhiro, Nogi Kiyoshi. Friction stir welding of a high carbon steel. Scripta Mater 2007;56(7):637–40.

[72]. Fujii H, Cui L, Tsuji N, Nataka K, Nogi K, Ikeda R, et al. Transformation in stir zone of friction stir welded carbon steels with different carbon contents. ISIJ Int 2007;47:299–306.

[73]. Fujii H, Ueji R, Takada Y, Kitahara H, Tsuji N, Nakata K, et al. Friction stir welding of ultrafine grained interstitial free steels. Mater Trans JIM 2006;47:239–42.

[74]. Reynolds AP, Tang W, Posada M, Deloach J. Friction stir welding of DH36 steel. Sci Technol Weld Join 2003;8:455–60.

[75]. Thomas WM, Threadgill PL, Nicholas ED. Feasibility of friction stir welding steel. Sci Technol Weld Join 1999;4:365–72.

[76]. Threadgill PL, Johnson R. Progress in friction stir welding of steels. Technical report 815/2004. Great Abington, Cambridge, UK: TWI (The Welding Institute); 2004.

[77]. Sanders DG, Ramulu M, Klock-McCook EJ, Edwards PD, Reynolds AP, Trapp T. Characterization of superplastically formed friction stir weld in titanium 6Al–4V: preliminary results. J Mater Eng Perform 17:187–92.

[78]. Maynier Ph, Jungmann B, Dollet J. Creusot–Loire system for the prediction of the mechanical properties of low alloy steel products. In: Doane DV, Kirkaldy JS, editors. Hardenability concepts with applications to steels. Materials Park, OH, USA: TMS–AIME; 1978. p. 518–45.

[79]. Konkol PJ, Mathers JA, Johnson R, Pickens JR. Friction stir welding of HSLA-65 steel for shipbuilding. J Ship Prod 2003;19:159–64.

[80]. Ueji R, Fujii H, Cui L, Nishioka A, Kunishige K, Nogi K. Friction stir welding of ultrafine grained plain low-carbon steel formed by the martensite process. Mater Sci Eng A 2006;423:324–30

[81]. Ozekcin A, Jin HW, Koo JY, Bangaru NV, Ayer R, Vaughn G, et al. A microstructural study of friction stir welded joints of carbon steels. Int J Offshore Polar Eng 2004;14:284–8.

[82]. Don-Hyun Choi.et al. "Hybrid Friction Stir Welding of High-carbon Steel". J. Mater. Sci. Technol., 2011, 27(2), 127-130.

[83]. Fujii.et al. "Friction stir welding of carbon steels". Materials Science and Engineering A 429 (2006) 50–57.

[84]. A.K Lakshminarayanan , V.Balasubramanian , M.Salahuddin. "microstructure tensile and impact toughness properties of Friction Stir Welded Mild Steel". Journal Of Iron And Steel Research, International. 2010, 17(10): 68-74.

[85]. M. Ghosh, K. Kumar, R.S. Mishra. "Friction stir lap welded advanced high strength steels: Microstructure and mechanical properties". Materials Science and Engineering A 528 (2011) 8111– 8119.

[86]. L. Y. WEI AND T. W. NELSON. "Correlation of Microstructures and Process Variables in FSW HSLA-65 Steel". Welding journal. 96-s May 2011, Vol. 90.

[87]. R. Johnson, P.L. Threadgill, in: S.A. David, T. DebRoy, J.C. Lippold, H.B. Smartt, J.M. Vitek (Eds.), Proceedings of the Sixth International Conference onTrends inWeldingResearch, PineMountain,GA,ASMInternational, 2003, pp.88–92.

[88]. M. Posada, J. Deloach, A.P. Reynolds, J.P. Halpin, in: S.A. David, T. DebRoy, J.C. Lippold, H.B. Smartt, J.M. Vitek (Eds.), Proceedings of the Sixth International Conference on Trends in Welding Research, Pine Mountain, GA, ASM International, 2003, pp. 307–312.

[89]. P.J. Konkol, J.A. Mathers, R. Johnson, J.R. Pickens, in: Proceedings of the Third International Symposium on Friction Stir Welding, Kobe, Japan, September 2001.

[90]. A.P. Reynolds, W. Tang, M. Posada, J. Deloach, Sci. Technol. Weld. Joining 8 (6) (2003) 455.

[91]. Sterling CJ, Nelson TW, Sorensen CD, Steel RJ, Packer SM. Friction stir welding of quenched and tempered C–Mn steel. Materials Park, OH, USA: TMS–AIME; 2003. p. 165–71.

[92]. W.M. Thomas, P.L. Threadgill, E.D. Nicholas, Sci. Tech. Weld. Joining 4 (1999) 365.

[93]. T.J. Lienert, J.E. Gould, in: Proceedings of the First International Symposium on Friction Stir Welding, Thousand Oaks, CA, USA, June 1999.

[94]. T.J. Lienert, W.L. Stellwag Jr., B.B. Grimmett, R.M. Warke, Weld. J. 82 (1) (2003) 1s.

[95]. A.P. Reynolds, M. Posada, J. Deloach, M.J. Skinner, J. Halpin, T.J. Lienert, in: Proceedings of the Third International Symposium on Friction Stir Welding, Kobe, Japan, September 2001.

[96]. Posada M, DeLoach JJ, Reynolds AP, Fonda RW, Halpin JP. Evaluation of friction stir welded HSLA-65. In: Proceedings of the fourth international friction stir welding symposium. Abington, UK: TWI; 2003.

[97]. S.H.C. Park, Y.S. Sato, H. Kokawa, K. Okamoto, S. Hirano, M. Inagaki, Scripta Mater. 49 (2003) 1175.

[98]. Chatterjee S, Wang HS, Yang JR, Bhadeshia HKDH. Mechanical stabilisation of austenite. Mater Sci Technol 2006;22:641–4.

[99]. R. Nandan.et.al. Recent advances in friction-stir welding – Process, weldment structure and properties. Progress in Materials Science 53 (2008) 980–1023

[100]. C.J. Sterling, T.W. Nelson, C.D. Sorensen, R.J. Steel, S.M. Packer, in: K.V. Jata, M.W. Mahoney, R.S. Mishra, S.L.Semiatin, T. Lienert (Eds.), Friction Stir Welding and Processing II, TMS, 2003, pp. 165–171.

[101]. Speich GR, Cuddy LJ, Gordon CR, DeArdo AJ. Formation of ferrite from control-rolled austenite. In: Marder AR, Goldstein JI, editors. Phase transformations in ferrous alloys. Warrendale, PA, USA: TMS–AIME; 1984. p. 341–89.

[102]. Konkol PJ, Murczek MF. Comparison of friction stir weldments and submerged arc weldments in HSLA-65 steel. Weld J Res Suppl 2007;86:187s–95s.

[103]. Konkol PJ. Characterisation of friction stir weldments in 500 brinell hardness quenched and tempered steel. In: Proceedings of the fourth international friction stir welding symposium. Abington, UK: TWI; 2003.

[104]. Mishra S, DebRoy T. A heat transfer and fluid flow based model to obtain a specific weld geometry using various combinations of welding variables. J Appl Phys 2005; 98(4).

Table.1: **Selection of process parameter [58].**

| Parameter	Range	Macrostructure	Observation
Rotational speed	< 800 rpm		Tunnel defect - Insufficient material transportation due to lesser frictional heat
	>1200 rpm		Tunnel defect and flash formation - excessive release of stirred materials to the upper surface, which resultantly left voids in the stir zone and formation of flash due to higher rotational speed.
Traverse speed	< 30 mm/min		Root Sticking due to excessive contact time between the hot weld metal and the steel backing plate. Also caused thermal damage to the tool.
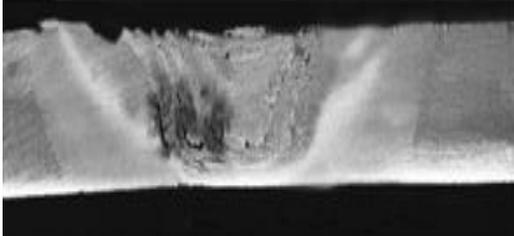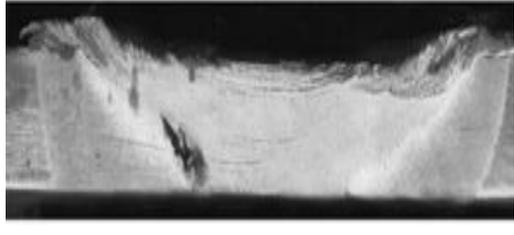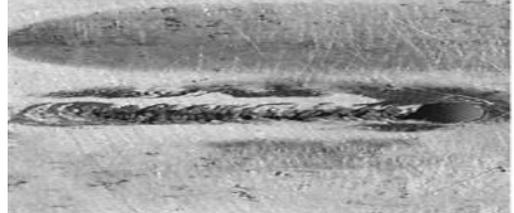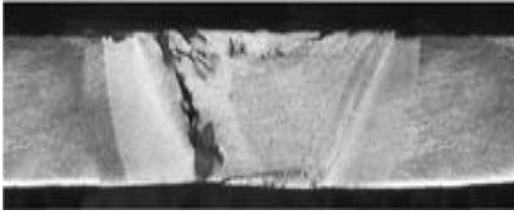
	>110 mm/min		Groove defect - Insufficient frictional heat hinders the viscoplastic material flow. Also high flow stresses in the Material can cause the tool to fail.
Shoulder Diameter	<16 mm		Surface defect - The area between the shoulder diameter and pin diameter is reduced which in turn reduced the material flow from the leading to trailing edge.
	> 24 mm		Tunnel Defect - Excessive Heat Generation and inadequate Material flow and mixing.
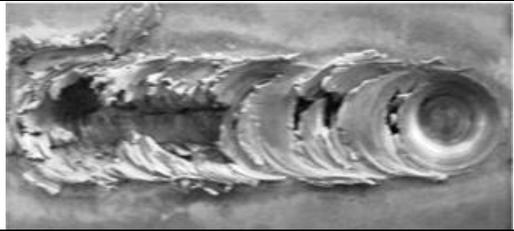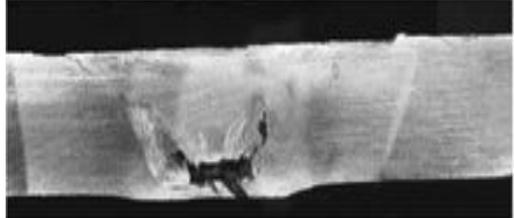
Table.2: FSW parameters and tool materials for FSW of steels [15]

Materials to be welded	Plate thickness (mm)	Tool rotation rate (rpm)	Tool traverse speed (mm/min)	Tool materials	References
SK5	4	700	80	WC-Co	[82]
IF steel, S12C, S35C	1.6	400	100–400	WC	[83]
AISI 1018 steel	5	1000	50	tungsten based alloy	[84]
AISI 409M ferritic stainless steel	4	800-1200	30-110	tungsten based alloy	[58]
M190 martensitic steel	1	1000	12.6 – 101.4	composite tool-DENSIMET-180 & CY-16	[85]
ASTM A945	9.5	300-600	51-203	PCBN (polycrystalline cubic boron nitride).	[86]
304L, 316L	5, 10	300–700	150, 180	W	[87]
HSLA-65	6.4, 12.7	400–450	99–120	W	[89]
DH-36	6.4	-	102–457	W alloy	[88,90]
C–Mn	6.4	-	-	Polycrystalline cubic boron nitride	[91]
12% Cr steel	12	-	240	-	[92]
AISI 1010	6.4	450–650	25–102	Mo and W-based alloys	[93,94]
304L	3.2, 6.4	300, 500	102	W alloy	[95,96]
304	6.0	550	78	Polycrystalline cubic boron	[97]

Note: This table is an update of values listed in FSW parameters and tool materials for FSW of steels [15].

Table: 3 **Chemical composition and Hardness predicted during FSW of steels [99]**

S.I.No	C	Si	Mn	Ni	Mo	Cr	V	OTHERS	HARDNESS [HV]			REFERENCE
									Plate	HAZ	TMAZ	
1	0.01	0.38	1.09	0.55	0.03	11.2	0.01	Nb 0.27	158	280	230	[75]
2	0.10	0.16	0.69	0.08	0.01	0.06	-		131	149	158	[75]
3	0.002		0.10					Ti 0.04	90	100	130	[73,83,72]
4	0.12		0.29						110		130[160]	[83,72]
5	0.21	0.24	0.50						125		230[500]	[72]
6	0.34	0.21	0.69					Cu0.01	155		280[360]	[83,72]
7	0.50	0.20	0.70					Cu0.01	200		360[520]	[72]
8	0.18		0.82						135		165	[48]
9	0.10	0.20	1.4					Cu0.22	180		200	[79]
10	0.18	0.30	1.25			0.08	0.35		175		320	[74]
11	0.14	0.02	0.64			0.08	0.35		280-460		150	[80]
12	0.13	0.26	1.52	0.03	0.17	0.03	0.06		200		300	[81]
13	0.32	0.35	1.20	0.20	0.65	1.30	0.056	B 0.0025	250		360	[81]
14	0.32	0.35	1.20	0.20	0.65	1.30	0.05	B 0.0025	250		450	[81]
15	0.84	0.17	0.4					0.017 P, 0.003 S	200	750-850	-	[82]
16			0.1					0.01P, 0.04Ti	70-90	110-140	-	[83]
17	0.12		0.29					0.01P,0.02S	100-130	130-170	-	[83]
18	0.34	0.21	0.69					0.01P, 0.01Cu	160-180	200-280	-	[83]
19	0.188	0.17	0.47	0.01	0.003	0.04		0.02CU	430±5	150-250	-	[85]
20	0.081	0.2	1.43	0.35	0.063	0.15	0.055	0.26Cu	90-130	200-205	-	[86]

Note: This table is an update of values listed in Compositions of steels (wt.%) in FSW welds [99].

Table.4: **Transverse tensile properties of FSW welds in various steels at room temperature [15]**

Materials	Conditions	UTS (MPa)	YS (MPa)	Elongation (%)	References
SK5	Base metal	610	-	-	[82]
	FSW welds	610	-	12-13	
IF	Base metal	288	155	92	[83]
	FSW welds	300-320			
S12C	Base metal	317	202	76	

	FSW welds	400-490			
S35C	Base metal	533	327	57	
	FSW welds	650-780			
AISI 409M	Base metal	536	364	31	[58]
	FSW welds				
AISI 1018	Base metal	421	361	27	[84]
	FSW welds	457	424	20	
M190	Base metal	1192±27	1030±27	14.3±1.4	[85]
	FSW welds	414-500	284-360	-	
12% Cr steel	Base metal	-	-	-	[92]
	FSW welds	539-541	-	-	
AISI 1010	Base metal	463	310	33.9	[93,94]
	FSW welds	476	331	22	
304L	Base metal	483	172	-	[87,96]
	FSW welds	621	340	-	
DH-36	Base metal	579	428	-	[96]
	FSW welds	624	566	-	
HSLA-65	Base metal	537	448	20	[89]
	FSW welds	569	493	30	
C–Mn steel	Base metal	248	204	9.5	[91]
	FSW welds	179	151	2.6	

Note: This table is an update of values listed Transverse tensile properties of FSW welds in various steels at room temperature [15].
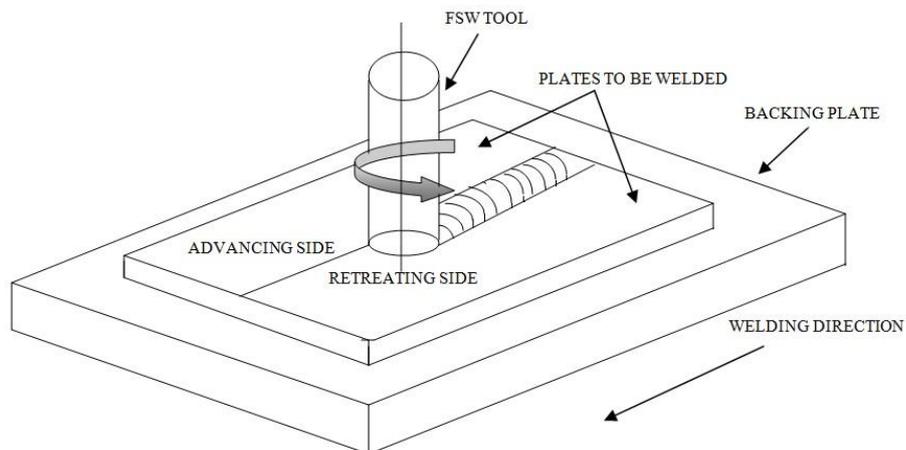
Fig.1: Friction-stir welding process
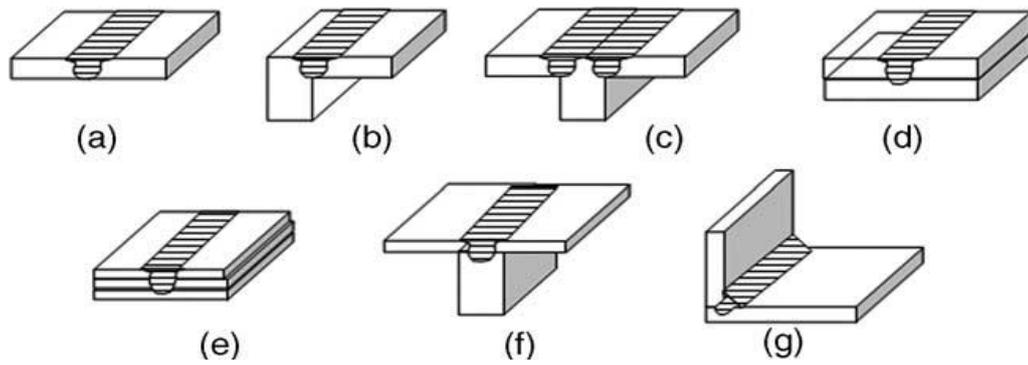
Fig.2: Types of joints (a) square butt, (b) edge butt, (c) T butt joint, (d) lap joint, (e) multiple lap joint, (f) T lap joint, and (g) fillet joint [15]
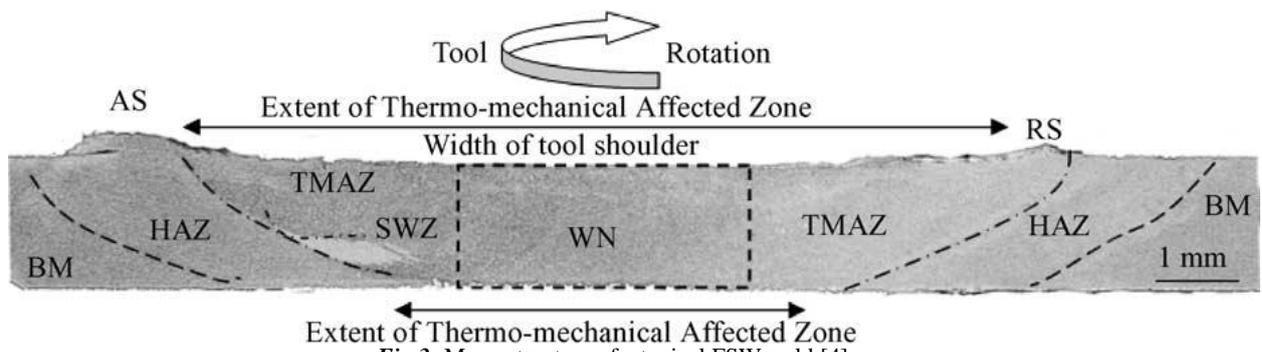
Fig.3: Macrostructure of a typical FSW weld [4]

| (a) | (b) | (c) | (d) |
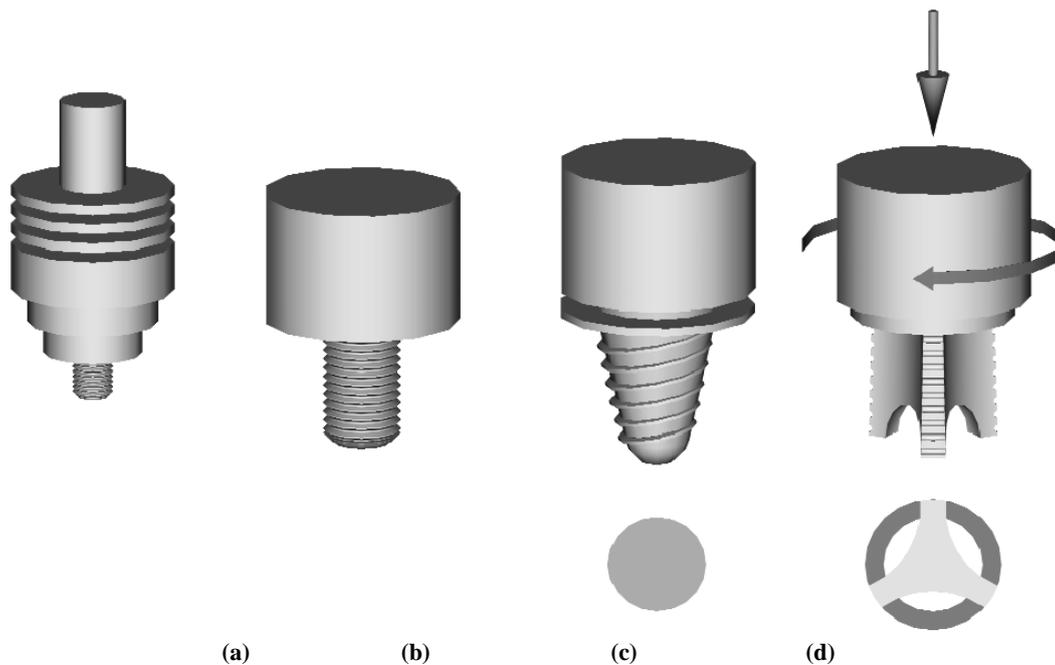
Fig.4: Friction stir welding tool shapes (a) stepped shoulder with cylindrical threaded pin (b) Cylindrical threaded pin (c) tapered pin (d) flared-triflute pin [5, 11]
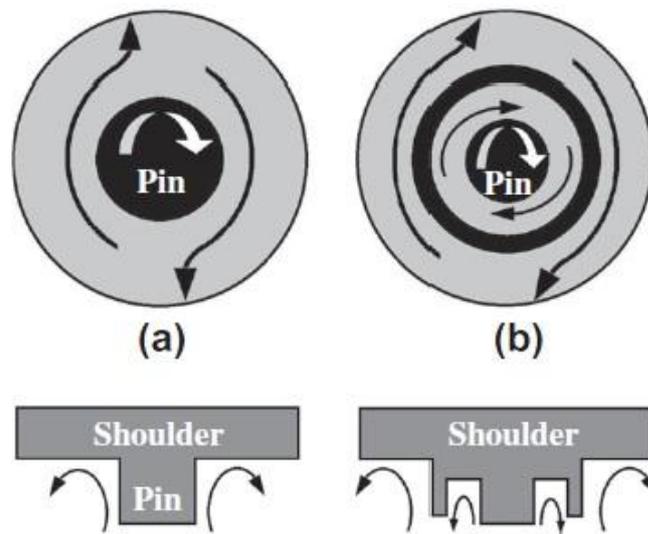
Fig. 5: Flow pattern of a (a) simple geometry (b) complex geometry [16]
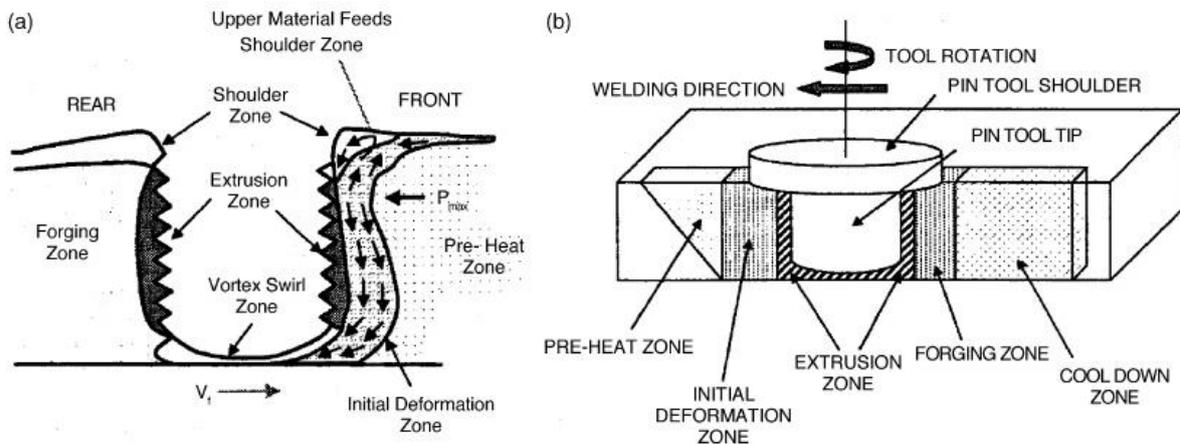
Fig.6: (a) Schematic representation of material flow (b) FSW metal working zones [7]
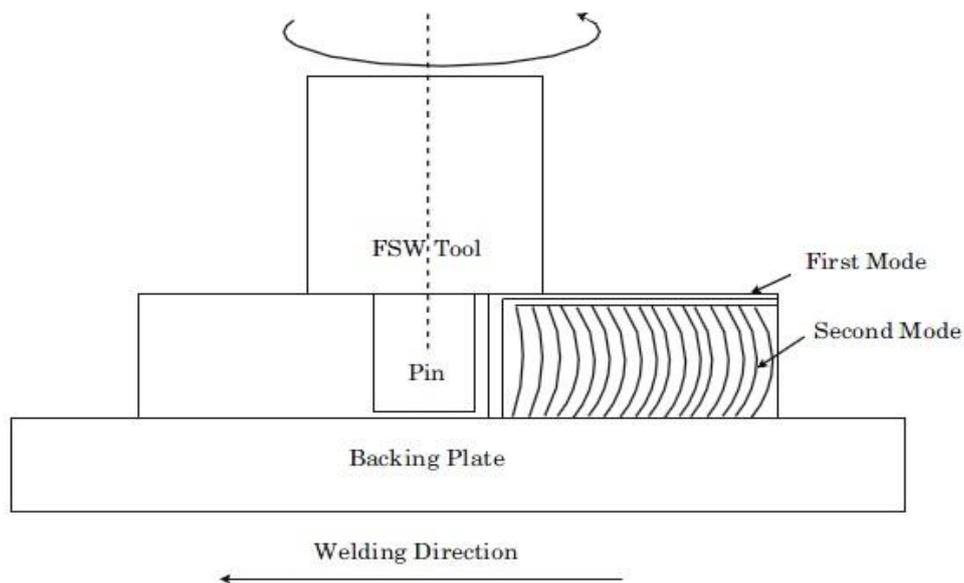
Fig.7: Schematic representation of two modes of metal transfer [9]
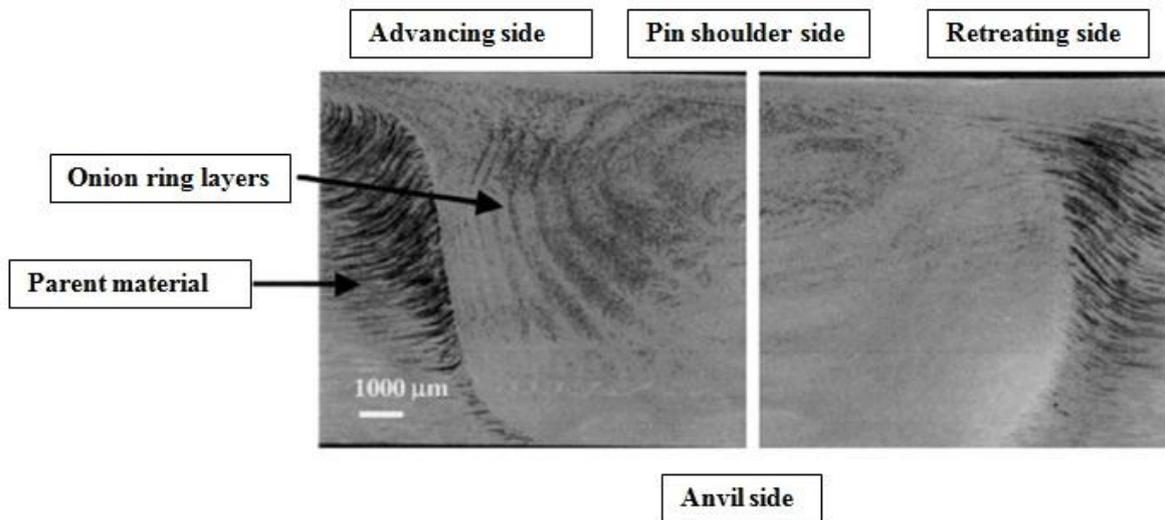
Fig.8: Schematic representation of onion ring pattern [26]
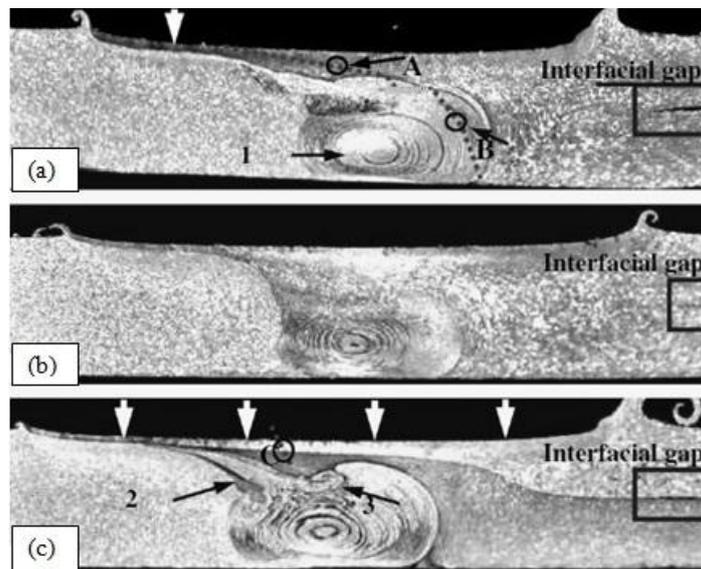
Fig.9: Cross-sections of the lap–butt joints under different pin off-sets (t values) towards RS of overlap AA5052 plates: (a) t = 0, (b) t = 0.5 mm, (c) t = 1.0 mm [16]
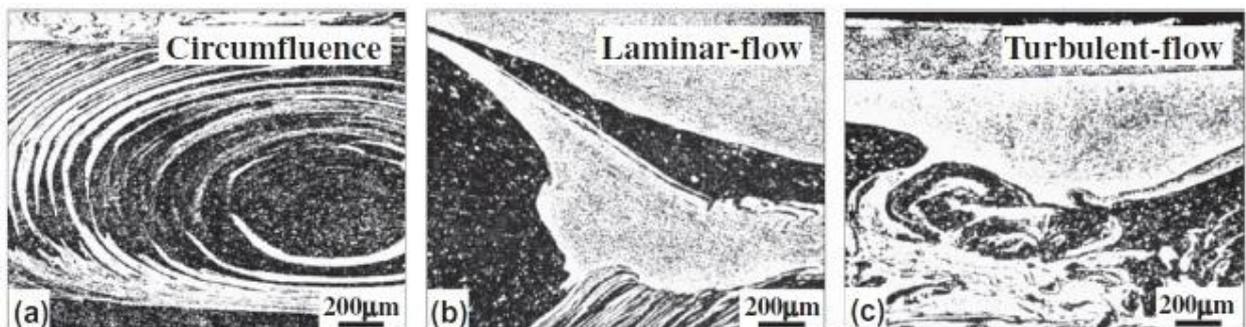

Fig.10: OM images of microstructures in the weld cross-sections (a) position '1' in Fig. 9a; (b) position '2' in Fig. 9c; (c) position '3' in Fig. 9c. [16]
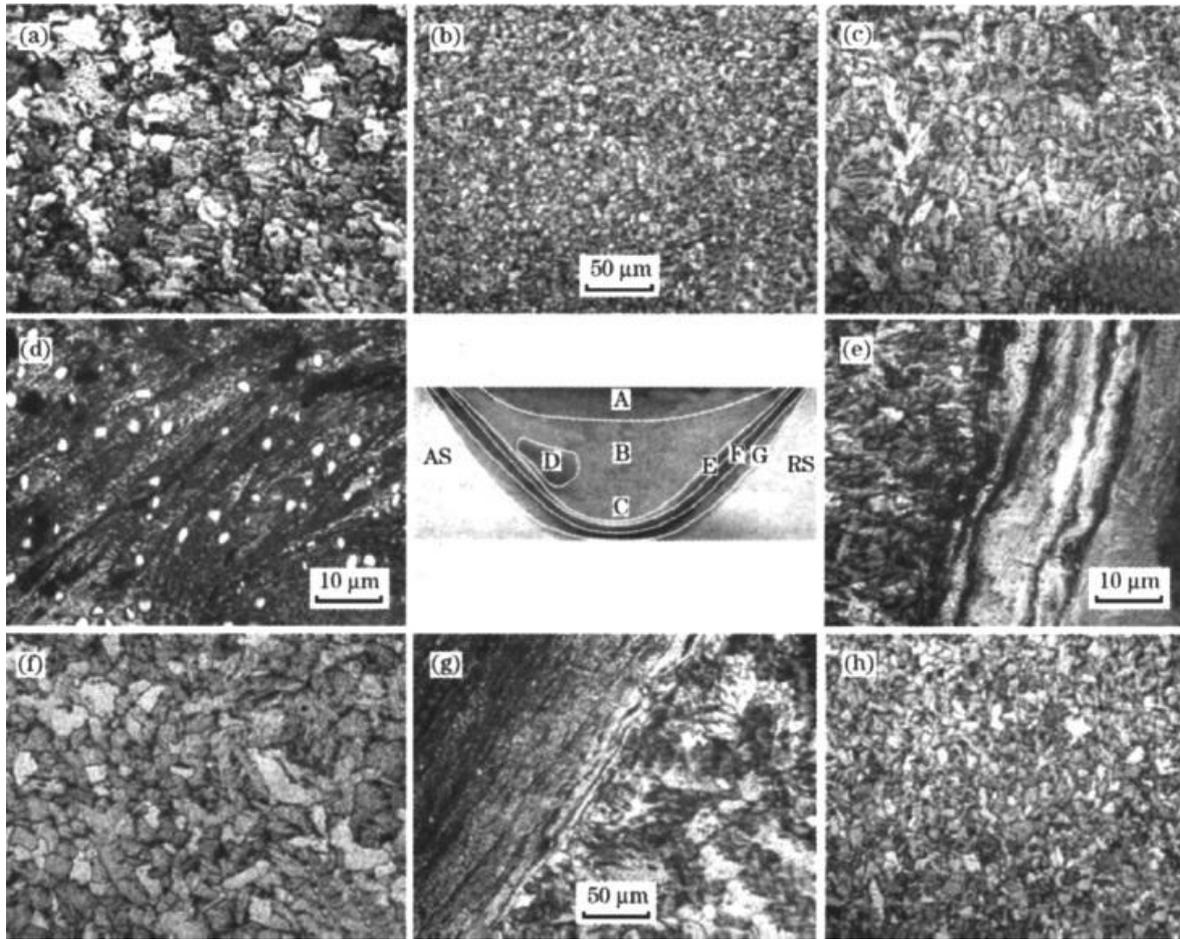
a) Base metal; (b) Top of stir zone (Region A); c) Middle of stir zone (Region B); (d) Swirl zone (Region D); (e) TMAZ (Region E); (f) FGHAZ-CGHAZ; (g) Interface SZ-HAZ; (h) Bottom of stir zone (Region c).
Fig.11: Optical micrographs of various regions of friction stir welded mild steel [84]
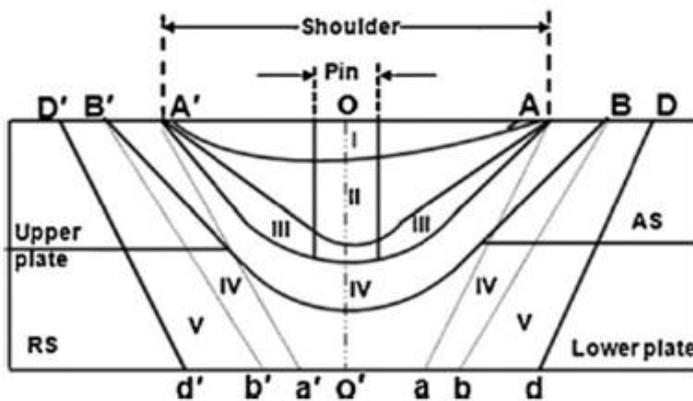
*OO' imaginary weld centre line
*Temperature between AA' : $\gg A_3$
*Temperature between B'A' and AB, i.e. HAZ-1: A_1 to A_3
*Temperature between D'B' and BD, i.e. HAZ-2 < A_1

Fig. 12: Schematic representation of different regions of friction stir welded M190 steel (not to scale) [85]
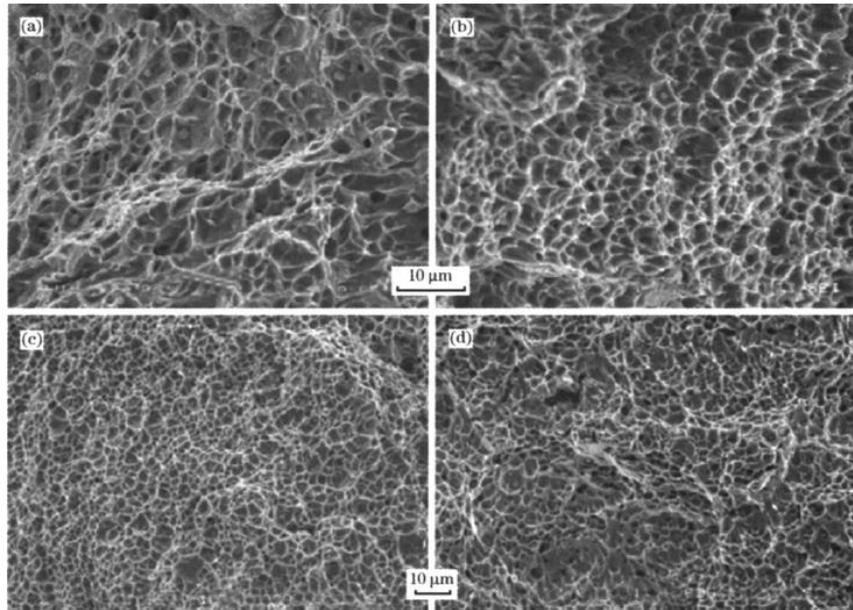
(a) Tensile specimen of base metal ;(c) Tensile specimen of FSW joint; (b) Impact specimen of base metal; (d) Impact specimen of FSW joint.

***Fig.13*:** SEM fractographs of tensile and impact specimens [84]